

Anisotropic interaction rules in circular motions of pigeon flocks: An empirical study based on sparse Bayesian learning

Duxin Chen,¹ Bowen Xu,¹ Tao Zhu,¹ Tao Zhou,² and Hai-Tao Zhang^{1,*}

¹Key Laboratory of Image Processing and Intelligent Control, School of Automation, State Key Laboratory of Digital Manufacturing Equipments and Technology, Huazhong University of Science and Technology, Wuhan 430074, P.R. China

²Web Sciences Center, University of Electronic Science and Technology of China, Chengdu 610054, P.R. China

(Received 5 April 2017; published 22 August 2017)

Coordination shall be deemed to the result of interindividual interaction among natural gregarious animal groups. However, revealing the underlying interaction rules and decision-making strategies governing highly coordinated motion in bird flocks is still a long-standing challenge. Based on analysis of high spatial-temporal resolution GPS data of three pigeon flocks, we extract the hidden interaction principle by using a newly emerging machine learning method, namely the sparse Bayesian learning. It is observed that the interaction probability has an inflection point at pairwise distance of 3–4 m closer than the average maximum interindividual distance, after which it decays strictly with rising pairwise metric distances. Significantly, the density of spatial neighbor distribution is strongly anisotropic, with an evident lack of interactions along individual velocity. Thus, it is found that in small-sized bird flocks, individuals reciprocally cooperate with a variational number of neighbors in metric space and tend to interact with closer time-varying neighbors, rather than interacting with a fixed number of topological ones. Finally, extensive numerical investigation is conducted to verify both the revealed interaction and decision-making principle during circular flights of pigeon flocks.

DOI: [10.1103/PhysRevE.96.022411](https://doi.org/10.1103/PhysRevE.96.022411)

I. INTRODUCTION

Collective motions in natural biological systems range from microscopic to macroscopic levels, such as bacterial colonies [1], migrating cells [2], insect swarms [3], fish schools [4], bird flocks [5], and even mammal herds [6,7]. To understand the underlying interaction mechanism of social animals, collective motion analysis has been extensively explored in recent years, which is continuing to attract increasing attention from biologists, physicists, life scientists, and computer scientists [8]. Dating back to several decades ago, simple interaction rules propelling individual agents have been proposed, which are sufficiently realistic to reproduce numerous observed phenomena and hence are beneficial for developing a methodology for better understandings of the system complexity consisting of many collectively self-propelled entities [8]. As a milestone study, Vicsek *et al.* proposed a well-known flock model, where each agent's direction of movement is determined by the average direction of the neighbors within a metric space. The so-called Vicsek model (VM) [9] captures the behavior of highly ordered structures that emerge in animal grouping motions. Following the research line, Tian *et al.* [10] investigated the optimal view angle in collective dynamics based on the VM, and Gao *et al.* [11] suggested that angle restriction enhances synchronization of self-propelled particles. Both of them [10,11] introduced the anisotropic interaction rules in numerical studies of coordinated behaviors. Another well-known study of Couzin *et al.* [12] proposed a three-sphere model with the consideration of blind visual fields that yields three typical patterns of universal collective motions in fish schools, i.e., swarm, torus, and migration states. Additionally, from the analytical point of view, a general theoretical framework describing the dynamics of biological

group behaviors was presented by Olfati-Saber *et al.* [13], which provides some insights into the emergence of highly coordinated collective behaviors yielded by simple interagent attractive/alignment/repulsive interactions.

Thanks to the swift development of data acquisition technology, not only numerical studies but also empirical investigations have been conducted to understand the varying underlying interindividual interaction principles and the matters triggering transition from nonequilibrium to equilibrium phases [8]. Recently, Ballerini *et al.* [14] proposed an alternative possibility for interaction rules in a huge flock comprising thousands of starlings, where it was observed that each bird interacted with only a fixed number of topological neighbors, instead of individuals within a specific metric distance. This model provided an explanation of the interaction mechanism among starlings, which was later reinforced by theoretical analysis [15] and interspecies experiments in mosquitofish schools [16]. With the assistance of GPS tracking device, Dell'Arciccia *et al.* [17] studied homing pigeons (*Columba livia*) and found that the homing performance of birds flying in a flock was significantly more coordinated than that of birds released individually. In addition, using high-resolution GPS data obtained from pigeon flocks, a hierarchical leadership network was revealed by Nagy *et al.* [18], where each pigeon acts as a leader or a follower, or plays a dual role when situated on middle layers. To investigate whether pigeon flocks obey a hierarchical or egalitarian interaction pattern, Zhang *et al.* [19] explored free flights of pigeon flocks and indicated that each pigeon tends to follow the average of its neighbors while moving along a smooth trajectory, whereas it switches to follow the leaders upon sudden turns or zigzags occur. Later, Chen *et al.* [20] reanalyzed the same homing flight datasets [18] and indicated that a pigeon flock has a fixed long-term leader for smooth moving trajectories in homing flights, whereas the leadership passes to a temporary one on sudden turns or zigzags. To investigate the principle governing self-organized

*zht@mail.hust.edu.cn

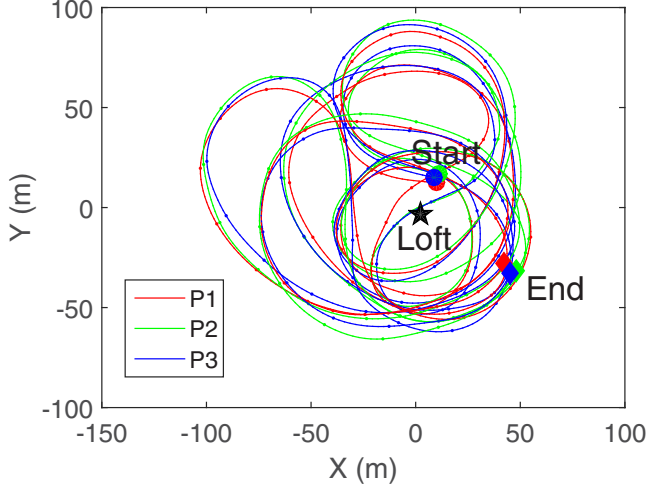


FIG. 1. Two-dimensional (2D) projection of the circular movement in flock A. To avoid confusion, only trajectories of three pigeons in the flock are exhibited as an illustration.

patterns, Ferrante *et al.* [21] developed an active-elastic-sheet method, which nicely explains the emergence of the ordered states of both natural and artificial swarms. Based on stereo imaging techniques, Attanasi *et al.* [22] obtained a high-resolution spatial dataset composed of thousands of starlings, which was afterwards used to formulate a realistic flocking dynamics model concerning spontaneous symmetry breaking and conservation rules. This model suggests that the information of directional turning propagates across the flock according to a linear dispersion law with negligible attenuation. Further, Mora *et al.* [23] introduced a dynamical inference technique based on the principle of maximum entropy to infer the strength and range of alignment forces from the datasets of flying starling flocks, which overcame the issue of slow experimental sampling rates. They found that local alignment emerges much faster than neighbor rearrangement. On the other hand, to understand the matters triggering phase transitions, Cheng *et al.* [24,25] reported that various pattern phase transitions can be captured in a minimal Hamiltonian model, with which one may predict the stability and tweak the morphology of the phases of self-propelled particles. From an engineering perspective, many of these aforementioned studies have provided specific insights into industrial applications of a huge volume of practical multi-agent systems, such as unmanned air vehicles [26] and multirobot formation control [27,28].

The objective of this study is to explore the underlying interindividual interaction rules and decision-making strategy in collective circular motions of small sized pigeon flocks. To this end, we focus on circular movements as shown in Fig. 1 and carry out a detailed investigation on high spatial-temporal resolution GPS datasets consisting of 30 releases of three pigeon flocks, each of which has ten individuals. We use the data of three pigeon flocks (labeled as flocks A, B, and C) with 30 releases from Ref. [29] (sampling period 0.1 s), each of which lasts from 2 to 7 min. The high-resolution GPS data were collected from free flights of pigeon flocks flying above the country area near Oxford. The GPS logger weighed 13 g, was based on a commercially available embedded GsmuILP device, logged time-stamped longitude, latitude, and altitude

data at 10 Hz. It was affixed to a pigeon's back with an elastic harness. Loggers were randomly allocated to pigeons before every flight. Due to the limitation of the GPS device in z axis and the average standard deviation of flight altitude in each release being sufficiently small (5.22 ± 1.27 m), it suffices to use the x - and y -axes data for investigation as the previous study [29] did, where they suggested that the accuracy of the x and y global coordinates was sufficient to carry out correlation analysis.

II. METHODS

First, a newly emerging machine learning method, namely Sparse Bayesian Learning (SBL) [30–33], is used to extract the interagent interaction among individuals. Different from the general machine learning theory [34], such as decision tree learning [35], support vector machine [36], and artificial neural network [37], SBL explores the sparse regression algorithms to learn from and make predictions on time-series data [30,38]. It employs strictly dynamical program instructions by building up a model from input data and thereby making data-driven prediction of the future evolution. Essentially, it relies on the assumption that captures the complex system dynamics by designing a finite set of dictionary functions which are used as *a priori* knowledge. Meanwhile, it adopts *a priori* probabilities to represent system uncertainty via probabilistic rules and inferential processes [31].

The massive data used in the SBL algorithm [33] is collected from the three flocks of free-ranging domestic pigeons flying above the country area near Oxford [29]. Each individual was equipped with a GPS logger to sample the longitude, latitude, and altitude data with 10 Hz sampling rate. Due to the inherent defects in the altitude data collected by the GPS device, we only focus on the two-dimensional planar data. Then we propose the following SBL formulation:

$$Y = \Phi\Omega + \xi, \quad (1)$$

where Y is the collected time-series data denoted in a state-space form; Φ is the dictionary function matrix, which gathers *a priori* knowledge of the input data with potential over-complete formulations; Ω is the coefficient matrix, including the objective connection information; and ξ is the additive process noise during the circular flights, which is assumed to be independent and identically distributed Gaussian distributed with zero mean [33]. More precisely, we pick $Y = \begin{bmatrix} \cdots & \cdots \\ x_i & y_i \\ \cdots & \cdots \end{bmatrix}_{q \times 2}$, where x_i and y_i are column vectors corresponding to the q -step input positional data in x axis and y axis; e.g., $x_i = [x_i(t-1), x_i(t-2), \dots, x_i(t-q-1)]^T$. Since the VM [9] is widely accepted in exploring collective motions of animal groups [8,14,39], we accordingly exhibit the details in the dictionary matrix $\Phi = \begin{bmatrix} \cdots & \cdots \\ M(x) & M(y) \\ \cdots & \cdots \end{bmatrix}$, i.e.,

$$[M(x)] = \begin{bmatrix} f_{j_1}(t-1) & \cdots & f_{j_{N-1}}(t-1) \\ f_{j_1}(t-2) & \cdots & f_{j_{N-1}}(t-2) \\ \vdots & \ddots & \vdots \\ f_{j_1}(t-q-1) & \cdots & f_{j_{N-1}}(t-q-1) \end{bmatrix}_{q \times 9}, \quad (2)$$

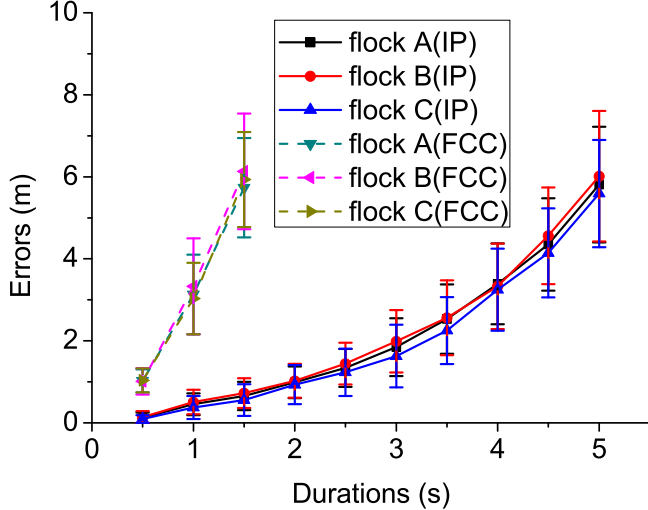


FIG. 2. Fitting errors of individual positions (IP) and filtered circular centers (FCC) corresponding to distinct recovered durations. Due to the fact that a flock of pigeons interact dynamically with switched neighbors, the fixed dictionary matrix cannot capture the time-varying interindividual interactions for a longer period. Thus, errors grow larger with increasing recovered durations.

with $f_{j_\lambda}(t) = x_{j_\lambda}(t) - x_i(t)$, such that $j_\lambda \neq i, \lambda = 1, 2, \dots, N-1$. Thus, the coefficient matrix has the form $\Omega = \begin{bmatrix} \omega_x & \omega_y \end{bmatrix}$. The sampling time is 0.1 s, and the subscript i only denotes the time step. M represents the compact form of the temporal regressive term. In Eq. (2), $f_{j_\lambda}(t) = x_{j_\lambda}(t) - x_i(t)$ means the position difference in x axis between individual i with all the others ($j \neq i$). Here, the element $M(x)$ is a $q \times 9$ matrix consisting of positional difference f_{j_λ} between the nine remaining individuals and the one to be recovered. Analogously, $M(y)$, a $q \times 9$ matrix, means the corresponding items in y axis. In the coefficient matrix, $[\omega_x, \omega_y]$ contains the connectivity information between individual i and the others. We then implement the SBL algorithm on every q step segment among the entire input data of 30 releases of three pigeon flocks. Obviously, such an interaction rule that individuals move towards the average position of neighbors with constant speed will drive them moving in a parallel phase [9,13]. Thus, the alignment of moving angles is indispensable for circular coordination. Since angular velocities are extremely small under the sampling rate 10 Hz, we hereby seek an equivalent transformation to investigate the relationships of circular centers of each individual by analogously employing a dictionary function matrix $[M(\tilde{x}), M(\tilde{y})]$, where \tilde{x} and \tilde{y} denote the Cartesian coordinates of the circular centers in x axis and y axis, respectively. Quantitatively, we show the evolution of fitting errors ($e = \sqrt{e_x^2 + e_y^2}$) of individual positions corresponding to distinct recovered durations in Fig. 2. It is observed that errors grow larger with increasing recovered durations, which is due to the fact that the fixed dictionary matrix cannot capture the time-varying interindividual interactions for a longer period, since a flock of pigeons interact dynamically with switched neighbors [18]. To investigate the underlying dynamical interaction rules of pigeon flocks, we

adopt the case $q = 5$, in which the errors are sufficiently small to guarantee the flock to adopt a fixed interaction network. Here, the fitting errors of circular centers for $q = 5$ are $e_x = 2.5340 \pm 27.1784(m)$ and $e_y = 2.4615 \pm 26.3144(m)$ (mean \pm SD). It should be noted that when individuals move straight in some consecutive instants, the circular centers reach infinity, which results in the unidentifiable cases and large values of standard deviation. By introducing an average filter with a threshold (100 m) on the circle radii, we recalculate the fitting errors of circular centers in the SBL algorithm for $q = 5$, which are $e_x = 1.0385 \pm 0.2503(m)$ and $e_y = 1.0101 \pm 0.3119(m)$ (mean \pm SD).

In general, supervised machine learning algorithm can be seen as minimizing the objective function which consists of a loss term and a regularization term, where the former can be square loss (the least-square method), hinge loss (support vector machine), exp-loss (boosting), log-loss (logistic regression), etc. By contrast, the latter, the regularization function, aims at constraining the model as simply as possible. Many options for selecting the regularization function exist, of which a monotonically increasing function of the model complexity is generally used, e.g., the following three types of norms, ℓ_0 -norm (the number of nonzero elements), ℓ_1 -norm (the sum of moduli of elements), and ℓ_2 -norm (the sum of the square roots). In this study, we solve the matrix multiplication (convex) optimization problem through a procedure relying on an efficient iterative reweighted ℓ_1 -minimization algorithm [40]. Compared with ℓ_0 and ℓ_2 methods, ℓ_1 regularization is neither easy to lead an NP-hard problem as ℓ_0 is, nor to obtain redundant solutions as ℓ_2 does [41]. In other words, ℓ_1 regularization can make the solution sparser and extract the minimal structures. We hereby adopt the ℓ_1 -minimization method as is used in exploring the underlying interaction mechanism in collective behaviors of fish schools [42], which can make the solution much sparser, and extract the minimal yet efficient connections. Afterwards, hyperparameters are utilized in marginal likelihood maximization, which uses prior distribution to distinguish themselves from the parameters of the underlying system model under analysis. Once the hyperparameters are determined, the solution is obtained by the maximum of a posterior estimation. Thus, we can acquire the posterior probability based on the Bayesian probability formula [33], posterior = $\frac{\text{likelihood} \times \text{prior}}{\text{marginal likelihood}}$, which leads the convergence to the most optimal cases. To implement the SBL method [33], we use the Matlab CVX package to solve the convex programming problems [43]. Thereby, we obtain the coefficient matrices $[\omega_x, \omega_y]$ and $[\omega_{\tilde{x}}, \omega_{\tilde{y}}]$, and extract the underlying interaction networks. The coefficient matrix Ω has a sparse structure with only dominant elements, while it may well fit the data. If the individual trajectory to be recovered is influenced by others, it is defined that these correlated individuals have directed connections to the one.

III. RESULTS

A. Intermittent alignment network

Based on the aforementioned SBL method [33], we investigate the network dynamics of the three pigeon flocks and exhibit the average degree distribution of the directed

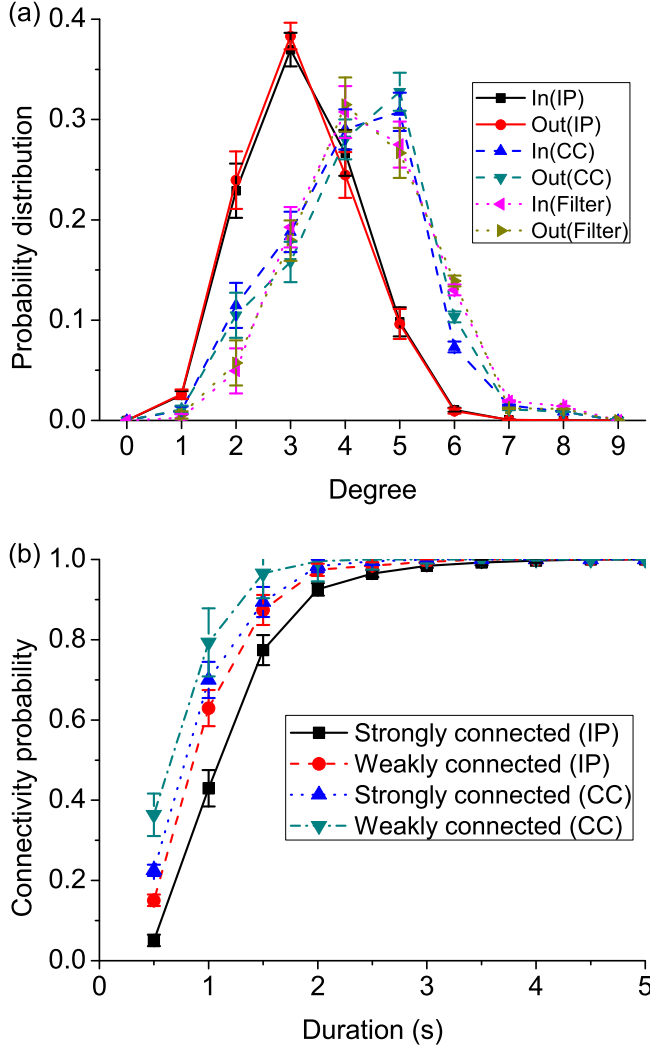


FIG. 3. Degree distribution and connectivity probability of interaction networks based on the SBL method for individual positions (IP), circular centers (CC), and filtered circular centers (Filter). (a) In and out degree distributions of the pigeon flocks. For each flock, individuals typically interact with a limited number of neighbors and never interact with all the other members. (b) Connectivity probability of the interaction networks. Durations indicate the number of consecutive instants of interaction networks merging into a union. Connectivity probability is calculated as the proportion of connected situations. Clearly, connectivity probability of both directed and undirected cases grow fast along increasing duration.

networks in Fig. 3(a). It is observed that the mostly encountered case is that each individual typically interacts with three neighbors by alignments of positions, whereas five neighbors by alignments of circular centers. Meanwhile, no pigeon interacts with all the other members in the flock. Due to the fact that pigeons interact with switched neighbors in an extremely short time instant, it suggests that pigeon flocks employ a local interaction mechanism and also suggests that the information achieved by one pigeon only propagates to just a few neighbors at one instant. Accordingly, we can predict only the local diffusive transmission of information propagating among pigeon flocks. The SBL algorithm [33]

extracts a directed relationship for a pair of pigeons. Here, a directed graph is called *weakly connected* if replacing all the directed edges with undirected edges produces a connected undirected graph. The term *strongly connected* is used if the network contains both a directed path from node u to node v and the reverse from v to u . In this study, both the weakly and strongly connected conditions of interaction networks are investigated. As shown in Fig. 3(b), a small possibility of connectivity is associated to the union of interaction networks within some consecutive instants. Evidently, the possibility grows larger with increasing interaction durations. It suggests that pigeon flocks employ a jointly connected interaction topology in free flights, where the instantaneous interaction networks do not keep connected, but the topology union of several continuous instants becomes connected. If we consider a sufficiently long period of time, a path will always exist in the union of the sequential instantaneous interaction networks from one individual to any other in the flock. The average number of neighbors is larger in the reconstruction of CC than the case of IP, although we have introduced an average filter on the circle radii. It is due to the fact that it is easy to recover IP, since the flock is relatively ordered. Note that the interlaced trajectories leading to the inconsistent CC results in the difficulty of identification in the SBL method [33].

B. Anisotropic interaction

For a flock of pigeons, individuals are not likely to establish connections with fixed neighbors in different releases. Neighbors are more likely to change when angular velocity is larger, due to the constraints of keeping cohesive with a low possibility of changing flight speed [44]. Thus, a natural question arises: how do pigeons choose their neighbors? A paradox has been existing in previous studies that bird flocks choose neighbors in terms of pairwise distances [9], and conversely they interact with a fixed number of neighbors in network topology [14]. Based on implementing the SBL method [33] on individual positions and circular centers, we show the average probability distribution of pairwise metric distances of neighbors corresponding to the three pigeon flocks in Fig. 4(a). Apparently, it is observed that there exists an inflection point on the evolution curves of the interacting distance, after which the interaction ratio decays strictly with increasing pairwise metric distances, and the maximum occurs within the range of 3–4 m with average interaction distance locating in the range of 5–6 m. Still, we show the probability distribution of pairwise metric distances of all the nine remainders (dash lines) in Fig. 4(a). The shifting of curves in positive x axis indicates that the focal individual tends to select interacting neighbors closer to itself. This initial low interaction probability is due to the fact that, within a short pairwise distance, individuals are more likely to avoid collision instead of alignment with its neighbor(s), which results in the lower distribution of remainders in short distance, and unidentified relationship extracted by the proposed SBL method. Additionally, the average anisotropy of interaction based on implementing the SBL method [33] on both individual positions and circular centers has been considered in Fig. 4(b). The circle center or the reference point represents the position of the focal

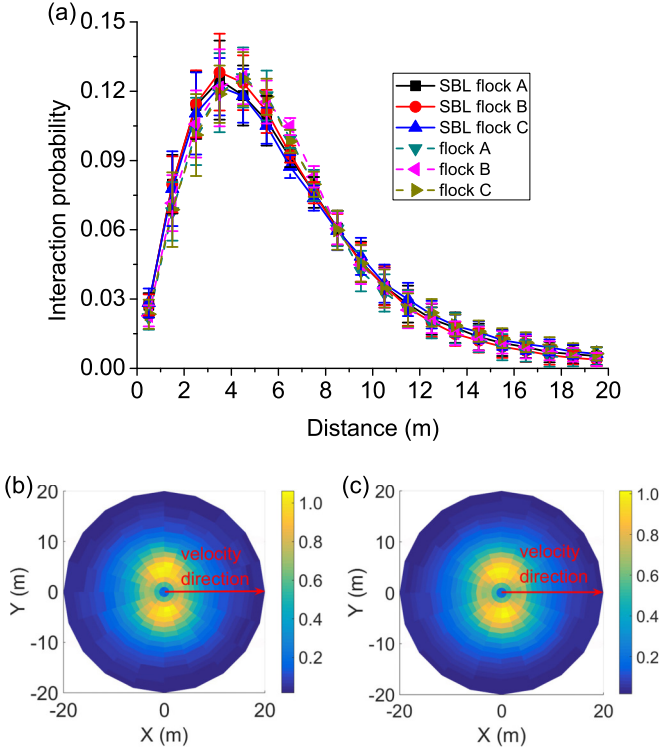


FIG. 4. (a) Probability distribution of pairwise metric distances of interacting neighbors (solid lines) and all the other individuals (dash lines) corresponding to the three pigeon flocks. The interaction probability distribution evolution curves have an inflection point, after which they decay strictly along increasing pairwise metric distances, whereas for the case of remainders including both interacting and noninteracting individuals, the curves have a shifting in the positive x axis, which means that interacting neighbors detected based on SBL are closer to the focal one. (b) Position distribution of interaction in flocks A, B, and C. The red arrow indicates the velocity direction, and colors demonstrate the normalized interaction frequencies. It is observed that individuals tend to interact with neighbors located right or left, but not along their velocity directions. (c) Position distribution of remainders in flocks A, B, and C. Analogously, we show the 360-degree position distribution of the remainders. It is observed that, on average, all the others locate on sides during circular motions.

individual at each time instant. Compared with the results in starling flocks [14], it is similarly observed that pigeons tend to interact with neighbors symmetrically located right or left, but not along their velocity directions. Inspired by the finding, we further exhibit the 360-degree position distribution of remainders including both interacting and noninteracting ones in Fig. 4(c). As expected, the natural average distribution is similarly anisotropic with higher proportions on sides. The observed anisotropic distribution of remainder individuals including both interacting and noninteracting ones can also be attributed to the physiological structure characteristics of birds and their anisotropic visual fields [45,46]. Thus, we suggest that in small-sized pigeon flocks, due to the anisotropic physiological visual fields, individuals are more likely to interact with closer neighbors on their left or right.

C. Theoretical model

Among abundant collective motion patterns of pigeon flocks, circular motion is a common yet fascinating behavior, where efficient and elaborate interagent interactions are required for coordination. Another feature is that the rotational direction undergoes regular periodical spontaneous changes, when a flock hovers near its home loft. To quantitatively refine the existing understanding of circular motions with spontaneous changes in rotational directions, we propose a self-propelled particle model based on a jointly connected interaction mechanism as below with the assistance of the findings endowed by the SBL method. Therein, three types of forces act on each particle, i.e., centripetal, alignment, and homing forces. The centripetal force is designed to drive each individual to rotate. The alignment force is the combination of neighboring forces to achieve the convergence to the circular centers. Considering the tendency of pigeons toward the roosting area [47], we use the homing force to yield attraction from the loft to each pigeon, which is designed as a piecewise convex function. The motions of individuals are mediated by the positions, velocities, and directions of their neighbors, as assumed in the VM [9]. Essentially, we employ a time-varying connectivity topology and apply a restriction on the communication capacity. In detail, for each individual, we randomly pick two to five individuals as its neighbors if there are more than four ones within its vision range. Note that as the intragroup connections become stronger with ascending neighborhood size, then collective motion is more rapidly achieved [48]. But this implies greater communication cost. Therefore, the proposed model with limited communication capacity establishes a balance between the coordination efficiency and the communication cost, which enables the verification of the feasibility of the inferred rules for reproducing coordinated circular motions. To focus on the crucial mechanism of intermittent interaction, the non-linear function related to the anisotropic visual apparatus has not been considered into the alignment force.

Now, based on the empirical results, we introduce the details of the proposed model. Consider a group of $n = 10$ units moving in a planar space, where each has a velocity in two-dimensional real space, i.e., $\vec{v}_i := [v_0 \cos \theta_i, v_0 \sin \theta_i]^T$, $v_i = \|\vec{v}_i\|$, where v_i and θ_i are the linear speed and direction of individual i . For conciseness, we omit the time variable t (e.g., $v_i = v_i(t)$). Let $\vec{p}_i := [x_i, y_i]^T$ be the particle's Cartesian coordinates. Recall that, the centripetal force will drive particle i to rotate independently. To generate the independent circular motion, each individual has the following dynamics:

$$\begin{aligned}\theta_i &= (\omega_i + \eta_\omega)dt, \\ dx_i &= (v_0 + \eta_v) \cos \theta_i dt, \\ dy_i &= (v_0 + \eta_v) \sin \theta_i dt,\end{aligned}\quad (3)$$

in which the centripetal force is ciphered, $v_0 = 20$ and $\omega_i = 0.5$ are the linear speed and angular speed assumed fixed in the numerical study, and η_v and η_ω denote the random noise ($\pm 10\%$) of the linear speed and angular speed, respectively.

Subsequently, the three types of forces are given through the following stochastic differential equation:

$$dv_i = (F_{\text{cen}} + F_{\text{align}} + F_{\text{home}})dt + \xi, \quad (4)$$

with ξ denoting a Poisson process, among which based on the empirical results that individuals interact with others by aligning their positions and moving angles, the alignment force F_{align} is derived from its neighbors in order to achieve the convergence of the motion centers. Thus, the alignment rule is defined as follows:

$$F_{\text{align}} = - \sum_{j \in N_i} \alpha(\|\vec{p}_{ij}\|) [\cos \theta_i \sin \theta_i] [f(x_{ij}) f(y_{ij})]^T, \quad (5)$$

with $i, j \in \{1, 2, \dots, n\}$ and $\|\vec{p}_{ij}\| = \|\vec{p}_i - \vec{p}_j\|$ denoting the Euclidean distance between individual i and j . It should be noted that the system dynamics is handled by discretization. Here, according to Fig. 4(a), we pick

$$\alpha(x) = \begin{cases} \omega_\alpha(x/\rho_1 - \rho_1/\rho_2), & 0 < x \leq \rho_1, \\ \omega_\alpha(1 - x/\rho_2), & \rho_1 < x \leq \rho_2, \\ 0, & x > \rho_2, \end{cases} \quad (6)$$

where $\omega_\alpha = 0.2$ is the weight of alignment, $\rho_1 = 8$ represents the pairwise distance corresponding to the largest interaction possibility, and ρ_2 denotes the range of alignment. To verify our understanding of the jointly connected topology employed by pigeon flocks, ρ_2 is defined as a triangular-wave function to introduce a time-varying interaction mechanism, which has a maximum and minimum positive amplitudes $\rho_m = 50$, and $\rho_1 = 8$, respectively, with frequency $\rho_F = 1/14$. A larger value of ω_α suggests a high rate of coordination. For circular motions, the unit alignment forces are calculated as $f(x_{ij}) = ax_{ij} + b\tilde{x}_{ij}$ and $f(y_{ij}) = cy_{ij} + d\tilde{y}_{ij}$, where $x_{ij} = x_i - x_j$, and \tilde{x}_{ij} means the position difference of circular centers of individuals i and j in x axis, i.e., $\tilde{x}_{ij} = v_i/\omega_i \sin \theta_i - v_j/\omega_j \sin \theta_j$, y_{ij} and \tilde{y}_{ij} are similarly defined in y axis. In the counterclockwise and clockwise cases, we pick $\begin{bmatrix} a & b \\ c & d \end{bmatrix} = \begin{bmatrix} 1 & -1 \\ 1 & 1 \end{bmatrix}$ and $\begin{bmatrix} a & b \\ c & d \end{bmatrix} = \begin{bmatrix} 1 & 1 \\ 1 & -1 \end{bmatrix}$, respectively.

The homing force F_{home} denotes the attraction from the loft to each particle [47], i.e.,

$$F_{\text{home}} = \begin{cases} \frac{1}{c_0} \left(\frac{\|\vec{p}_i - \vec{p}_0\|}{L} \right)^{\omega_\beta}, & \|\vec{p}_i - \vec{p}_0\| \geq L_0, \\ 0, & \|\vec{p}_i - \vec{p}_0\| < L_0, \end{cases} \quad (7)$$

where $L_0 = 40$ is a minimum radius of a circular homing area meaning that within the range $\|\vec{p}_i - \vec{p}_0\| < L_0$, individuals feel no attraction from the loft. Besides, $c_0 = 2.5e^{-6}$ is a constant, $\omega_\beta = 2.2$ denotes the attraction strength, $\vec{p}_0 := [x_0, y_0]^T$ is the Cartesian coordinates of the loft, and $L = 400$ is the side length for the simulation space. Low values of ω_β imply weak attraction from the loft, whereas an adsorption phenomenon emerges around the loft with higher values of ω_β .

As shown in Fig. 5, we exhibit the probability distributions of the system status, i.e., the directional index of the entire flock. We use signs “+” and “−” to represent the individual counterclockwise and clockwise rotations, respectively. Specifically, “±10” mean that the entire flock consisting of ten individuals rotates collectively in a counterclockwise or clockwise direction, respectively. With the reduction and increase of the index values, the entire flock gradually changes rotational direction from counterclockwise to clockwise and the reverse, respectively. The concave probability distribution of the system status indicates that more individuals change

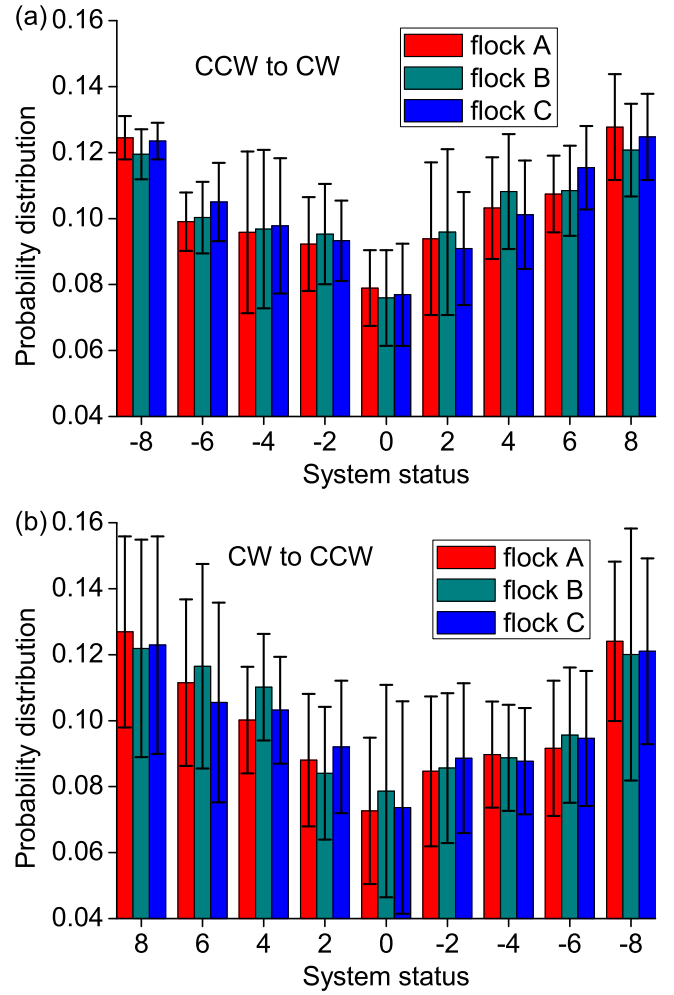


FIG. 5. Probability distributions of the system status, i.e., the directional index of the entire flock. Therein, the sign “+” and “−” represent the individual counterclockwise and clockwise rotations, respectively. With the reduction and increase of the index values, the entire flock gradually changes rotational direction from counterclockwise to clockwise and the reverse, respectively. Significantly, it is observed that the spontaneous changes of rotational directions follow a Gaussian distribution.

their rotational direction in the medium stage, whereas the number of directional switching pigeons reduces gradually in the earlier and later stages. Thus, it is reasonable to assume that spontaneous changes of rotational directions follow a Gaussian distribution. To explain how a heterogeneous flock of pigeons with varying stamina can achieve spontaneous changes of rotational direction in circular motions, we assume that every individual has a depletion time which follows Gaussian distribution. When a pigeon feels “tired” or wants to change the rotational direction but most of the others not, it must follow them unwillingly but with increasingly greater intension to change. Thus, when a sufficient number of willing members have been accumulated to change their rotational direction, they drive the entire flock to switch. Refer to the Supplemental Material video for simulation results [49] and the previous study [18] for realistic circular motions of pigeon flocks.

The main characteristic of circular motions by pigeon flocks is the highly synchronous state with unpredictable changes in rotational direction. As shown in Figs. 6(a)–6(c), another unique feature is that pigeons periodically rotate around their loft during the flight. When a collective decision is made to change rotational direction, the average positions corresponding to three continuous instants (which suffices to calculate a curvature) lie on a relatively straight line. Thus, the radius of the curvature suddenly increases, and hence the distance rises between the average circular center and the loft. To investigate more deeply into the principle underneath these behaviors, as shown in Figs. 6(a)–6(c), we compare the results of the present numerical study with the experimental data based on the trajectory containing both counterclockwise and clockwise circular motions. The former coincides well with the latter. In natural situation, pigeons fly in a three-dimensional space, so it makes sense to see staggered overlaps along the two-dimensional projected trajectory. Therefore, we do not consider repulsion forces due to the projecting overlap. Analogously, when governed by the three forces and the jointly connected topological mechanism in the proposed model as well as the decision-making strategy including compromise and the Gaussian distribution of depletion time, the individuals move collectively in circles with different radii. In addition, all of the pigeons change their rotational directions spontaneously, but never stray far from their loft.

IV. DISCUSSION

This study focuses on circular motions because a turning command is broadcasted through the flock on almost every occasion, whereas the alignment of velocity may carry significant directional information of real interactions [50,51]. Furthermore, based on the SBL method [33], it is observed that the interaction network of a pigeon flock is even almost always unconnected at each instant, whereas it becomes connected when the multiple networks are merged over sufficiently long consecutive time intervals. Thus, pigeon flocks employ a weakly connected principle to achieve coordination, and thereby substantially reducing the communication costs, which better explains actual intermittent communication phenomena observed in biological groups [5,7,52], and helps provide a biological evidence of the existence of jointly connected interactive network topology in bird flocks. Moreover, the jointly connected topology guarantees that each individual can communicate with others directly or indirectly during a sufficiently long time. However, what will happen if an agent escapes the influence of the others for a long period? In the present numerical study, by using a weaker jointly connected condition with a faster decay rate of ρ_2 , an individual far from the others becomes an outlier after a change in the movement direction, so it whirls constantly and spontaneously as observed in nature [18]. Therefore, to achieve collective coordination, the influence of the others should be sufficiently strong, especially under some crucial situations, such as the rotational direction switching time and the occurrence of conflicting decisions. In addition, it should be noted that we implemented both the empirical and numerical studies based on the widely used velocity alignment

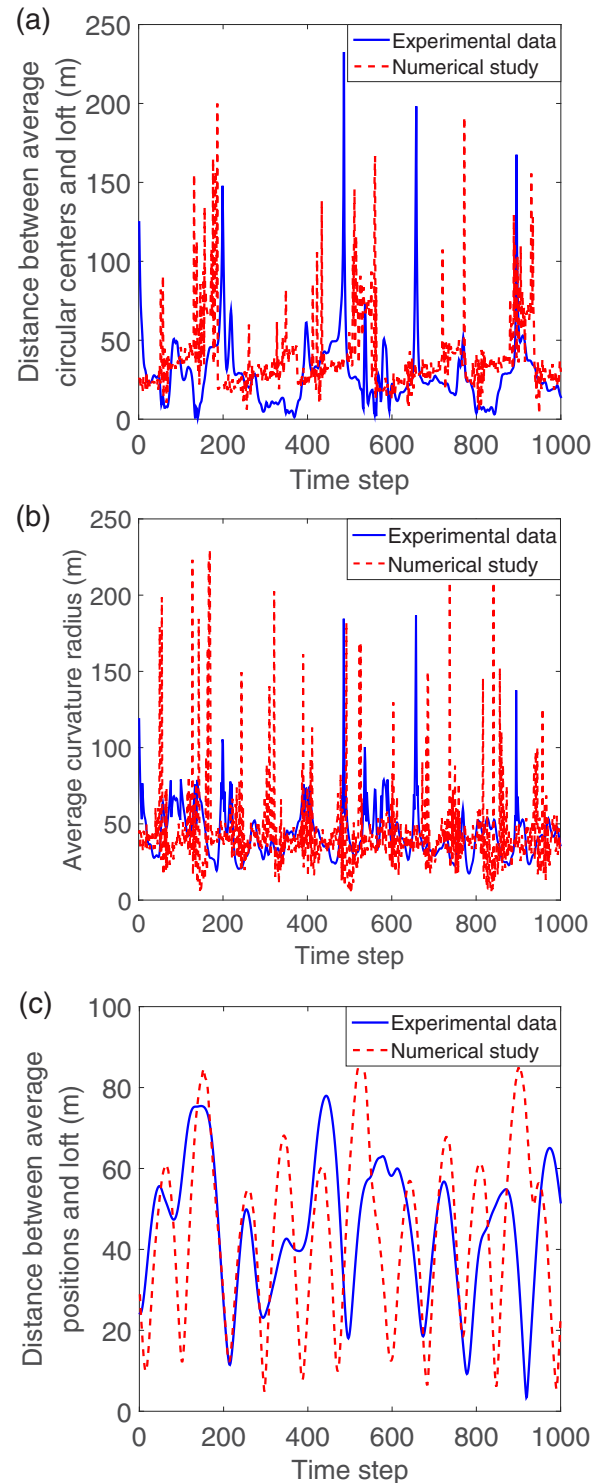


FIG. 6. Comparison between experimental data and numerical study results. 100-s long (1000 time steps) segment of flight trajectories from flock A. (a)–(c) The distances between the average circular centers and loft, average curvature radius, and distances between the average positions and loft, respectively. If the pigeon flock flies relatively straight for three consecutive instants, the average curvature radius will grow larger in synchronized manner with peaks in (a) and (b). The evolution tendency in numerical study is well consistent with the empirical data.

among self-propelled entities [9,12,51]. Other possibilities still exist, e.g., Barberis *et al.* [53] suggested that position-based active models with a vision limitation can exhibit various complex, large-scale and self-organized patterns, including the millinglike patterns found in fish. Although a centrifugal force is not needed to induce spontaneous rotation (a scattered distribution of individuals along the circle) [54], we still introduce a centripetal force for each individual to achieve the cohesively circular movements, and the independent rotation.

Group structure is the foremost fascinating result, yielded by interindividual interactions, or conversely, interactions are ciphered in the coordinated spatial structure [51]. To extract the underlying interaction rules, we seek assistance from the SBL method [30–33]. Based on empirical results, we observed that during coordinated circular flights, the interaction probability is strongly correlated with pairwise metric distance. It monotonously increases until reaches an inflection point at pairwise distance of 3–4 m, after which it decays strictly with rising pairwise metric distance. Further, compared with the natural distribution of remainders including both interacting and noninteracting ones, the larger average maximum probability (inflection point) 4–5 m indicates that individuals are more likely to interact with closer neighbors. Thus, we suggest that individuals in small-sized bird flocks reciprocally cooperate with a limited and time-varying number of neighbors in metric space, rather than interacting with a fixed number of distance-independent neighbors. Meanwhile, the density of spatial neighbor distribution is strongly anisotropic, with an

evident lack of interactions along individual velocity direction. It coincides with and may be deemed to the physiological characteristics and visual field of birds [45,46]. Another impressive scenario is the V-shape flight of ibis flocks [55], which is strongly anisotropic in spatial structure. With respect to the way for pigeon flocks to achieve coordination and synchronization, the revealed connectivity probability mechanism and the normally distributed decision-making strategy provide an explanation. In addition, we suggest that the SBL method helps discover the interaction mechanism from the perspective of a dynamical machine learning analysis in collective behaviors. In future research, it will be necessary to scale up from the current small-sized bird flocks to larger ones and to check the interspecies issue to other kinds of animal groups. How do they interact in coordinated movements? Will the density of spatial neighbor distribution still follow anisotropy? What are the specific anisotropic ranges in other gregarious animal groups? These fascinating questions merit further investigations.

ACKNOWLEDGMENTS

The work of H.-T. Zhang was supported by the National Natural Science Foundation of China under Grants No. 61673189 and No. 51535004, the Guangdong Innovative and Entrepreneurial Research Team Program under Grant No. 2014ZT05G304, and the HUST key Innovative Interdisciplinary Team Program under Grant 2016JCTD103.

-
- [1] A. Sokolov, I. S. Aranson, J. O. Kessler, and R. E. Goldstein, *Phys. Rev. Lett.* **98**, 158102 (2007).
 - [2] B. Szabo, G. J. Szöllösi, B. Gönci, Z. Jurányi, D. Selmecezi, and T. Vicsek, *Phys. Rev. E* **74**, 061908 (2006).
 - [3] J. Buhl, D. J. Sumpter, I. D. Couzin, J. J. Hale, E. Despland, E. R. Miller, and S. J. Simpson, *Science* **312**, 1402 (2006).
 - [4] D. J. Hoare, I. D. Couzin, J. G. Godin, and J. Krause, *Anim. Behav.* **67**, 155 (2004).
 - [5] I. L. Bajec and F. H. Heppner, *Anim. Behav.* **78**, 777 (2009).
 - [6] S. Gueron, S. A. Levin, and D. I. Rubenstein, *J. Theor. Biol.* **182**, 85 (1996).
 - [7] F. Ginelli, F. Peruani, M. H. Pillot *et al.*, *Proc. Natl. Acad. Sci. USA* **112**, 12729 (2015).
 - [8] T. Vicsek and A. Zafeiris, *Phys. Rep.* **517**, 71 (2012).
 - [9] T. Vicsek, A. Czirók, E. Ben-Jacob, I. Cohen, and O. Shochet, *Phys. Rev. Lett.* **75**, 1226 (1995).
 - [10] B. M. Tian, H. X. Yang, W. Li, W. X. Wang, B. H. Wang, and T. Zhou, *Phys. Rev. E* **79**, 052102 (2009).
 - [11] J. Gao, S. Havlin, X. Xu, and H. E. Stanley, *Phys. Rev. E* **84**, 046115 (2011).
 - [12] I. D. Couzin, J. Krause, R. James, G. D. Ruxton, and N. R. Franks, *J. Theor. Biol.* **218**, 1 (2002).
 - [13] R. Olfati-Saber, *IEEE T. Automat. Contr.* **51**, 401 (2006).
 - [14] M. Ballerini, N. Cabibbo, R. Candelier *et al.*, *Proc. Natl. Acad. Sci. USA* **105**, 1232 (2008).
 - [15] N. W. Bode, D. W. Franks, and A. J. Wood, *J. R. Soc. Interface* **8**, 301 (2010).
 - [16] J. E. Herbert-Read, A. Perna, R. P. Mann, T. M. Schaerf, D. J. Sumpter, and A. J. Ward, *Proc. Natl. Acad. Sci. USA* **108**, 18726 (2011).
 - [17] G. Dell’Ariccia, G. Dell’Omo, D. P. Wolfer, and H. P. Lipp, *Anim. Behav.* **76**, 1165 (2008).
 - [18] M. Nagy, Z. Ákos, D. Biro, and T. Vicsek, *Nature* **464**, 890 (2010).
 - [19] H. T. Zhang, Z. Chen, T. Vicsek, G. Feng, L. Sun, R. Su, and T. Zhou, *Sci. Rep.* **4**, 5805 (2014).
 - [20] D. Chen, T. Vicsek, X. Liu, T. Zhou, and H. T. Zhang, *Europhys. Lett.* **114**, 60008 (2016).
 - [21] E. Ferrante, A. E. Turgut, M. Dorigo, and C. Huepe, *Phys. Rev. Lett.* **111**, 268302 (2013).
 - [22] A. Attanasi, A. Cavagna, L. Del Castello *et al.*, *Nat. Phys.* **10**, 691 (2014).
 - [23] T. Mora, A. M. Walczak, L. D. Castello *et al.*, *Nat. Phys.* **12**, 1153 (2016).
 - [24] Z. Cheng, Z. Chen, T. Vicsek, D. Chen, and H. T. Zhang, *New J. Phys.* **18**, 103005 (2016).
 - [25] A. H. Travesinger, *Nat. Phys.* **12**, 992 (2016).
 - [26] R. W. Beard, T. W. McLain, M. A. Goodrich, and E. P. Anderson, *IEEE T. Robot. Autom.* **18**, 911 (2002).
 - [27] H. T. Zhang, Z. Chen, L. Yan, and W. Yu, *IEEE Trans. Contr. Sys. Tech.* **21**, 1416 (2013).
 - [28] G. Vásárhelyi, C. Virágh, G. Somorjai, N. Tarcai, T. Szorenyi, T. Nepusz, and T. Vicsek, in *Proceedings of the IEEE/RSJ International Conference on Intelligent Robots and Systems* (IEEE, Chicago, 2014), pp. 3866–3873.

- [29] M. Nagy, G. Vásárhelyi, B. Pettit, I. Roberts-Mariani, T. Vicsek, and D. Biro, *Proc. Natl. Acad. Sci. USA* **110**, 13049 (2013).
- [30] M. E. Tipping, *J. Mach. Learn. Res.* **1**, 211 (2001).
- [31] D. P. Wipf and B. D. Rao, *IEEE T. Signal Process.* **52**, 2153 (2004).
- [32] Z. Zhang and B. D. Rao, *IEEE J. Select. Topics Signal Process.* **5**, 912 (2011).
- [33] W. Pan, Y. Yuan, J. Gonçalves, and G. B. Stan, *IEEE T. Automat. Contr.* **61**, 182 (2016).
- [34] R. S. Michalski, J. G. Carbonell, and T. M. Mitchell, *Machine Learning: An Artificial Intelligence Approach* (Springer Science & Business Media, New York, 2013).
- [35] Y. Freund and L. Mason, in *Proceedings of the 16th International Conference on Machine Learning* (ICML, Bled, 1999), pp. 124–133.
- [36] J. A. K. Suykens and J. Vandewalle, *Neural Process. Lett.* **9**, 293 (1999).
- [37] J. J. Hopfield, *IEEE Circ. Device. Mag.* **4**, 3 (1988).
- [38] M. Barahona and C. S. Poon, *Nature* **381**, 215 (1996).
- [39] I. D. Couzin, J. Krause, N. R. Franks, and S. A. Levin, *Nature* **433**, 513 (2005).
- [40] D. L. Donoho and M. Elad, *Proc. Natl. Acad. Sci. USA* **100**, 2197 (2003).
- [41] I. Daubechies, R. DeVore, M. Fornasier, and C. S. Güntürk, *Commun. Pure Appl. Math.* **63**, 1 (2010).
- [42] S. B. Rosenthal, C. R. Twomey, A. T. Hartnett, H. S. Wu, and I. D. Couzin, *Proc. Natl. Acad. Sci. USA* **112**, 4690 (2015).
- [43] M. Grant, S. Boyd, and Y. Yuan (2008), retrieved from <http://cvxr.com>.
- [44] M. Yomosa, T. Mizuguchi, G. Vásárhelyi, and M. Nagy, *PLoS ONE* **10**, e0140558 (2015).
- [45] G. R. Martin, *J. Comp. Physiol. A* **159**, 545 (1986).
- [46] G. R. Martin and G. Katzir, *Brain. Behav. Evo.* **53**, 55 (1999).
- [47] F. Heppner and U. Grenander, in *The Ubiquity of Chaos*, edited by S. Krasner (AAAS, Washington, 1990), pp. 233–238.
- [48] Z. Chen and H. T. Zhang, *Automatica* **47**, 1929 (2011).
- [49] See Supplemental Material at <http://link.aps.org/supplemental/10.1103/PhysRevE.96.022411> for simulation results of circular motions.
- [50] W. Bialek, A. Cavagna, I. Giardina, T. Mora, E. Silvestri, M. Viale, and A. M. Walczak, *Proc. Natl. Acad. Sci. USA* **109**, 4786 (2012).
- [51] A. Cavagna, A. Cimorelli, I. Giardina, G. Parisi, R. Santagati, F. Stefanini, and M. Viale, *Proc. Natl. Acad. Sci. USA* **107**, 11865 (2010).
- [52] C. K. Hemelrijk and H. Hildenbrandt, *Interface Focus* **2**, 726 (2012).
- [53] L. Barberis and F. Peruani, *Phys. Rev. Lett.* **117**, 248001 (2016).
- [54] B. Ferdinandy, K. Ozogány, and T. Vicsek, *Physica A (Amsterdam)* **479**, 467 (2017).
- [55] S. J. Portugal, T. Y. Hubel, J. Fritz *et al.*, *Nature* **505**, 399 (2014).